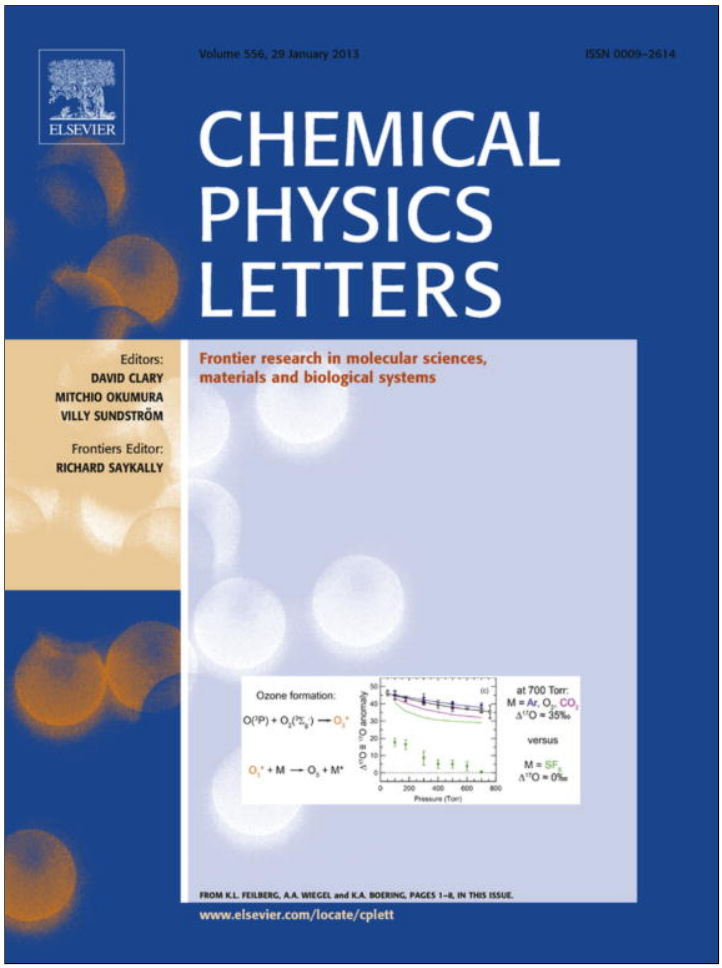

Chemical Physics Letters 556 (2013) 1–8

Contents lists available at SciVerse ScienceDirect

Chemical Physics Letters

journal homepage: www.elsevier.com/locate/cplett

FRONTIERS ARTICLE

Probing the unusual isotope effects in ozone formation: Bath gas and pressure dependence of the non-mass-dependent isotope enrichments in ozone

K.L. Feilberg [a], A.A. Wiegel [a], K.A. Boering [a,b,*]

[a] Department of Chemistry, University of California, Berkeley, CA 94720-1460, USA
[b] Department of Earth and Planetary Science, University of California, Berkeley, CA 94720, USA

ARTICLE INFO

Article history:
Available online 22 October 2012

ABSTRACT

Laboratory and atmospheric measurements of the isotopic composition of ozone have shown large and unusual 'non-mass-dependent' enrichments in ^{17}O and ^{18}O of ~10% relative to the O_2 from which it is formed. We present measurements of the bath gas and pressure dependence of the isotope enrichments in ozone formed by photolysis of O_2 in the presence of Ar, O_2, CO_2, and SF_6 from 50 to 760 Torr. The results provide new insights into the origin of the dynamically-driven symmetry-related isotope effect involved and new benchmarks for theory, including elimination of all isotope selectivity for ozone formation in SF_6 by 700 Torr.

1. Introduction

Unusual enrichments in the rare heavy oxygen isotopes in ozone were first discovered in the atmosphere [1–3] and in laboratory experiments [4–6] nearly 30 years ago. The isotope enrichments are unusual in two respects. First, the enrichments are surprisingly large, with ^{17}O and ^{18}O enrichments >10% above those expected from a statistical redistribution of isotopes in the reactant O_2 from which it is formed, versus more typical values for isotope enrichments or depletions of ~0.1–1% for elements heavier than hydrogen. Second, the isotope enrichments in ozone are distinctly 'non-mass-dependent' – that is, measurements of the ^{17}O and ^{18}O isotopic compositions of ozone fall far off the 'mass-dependent' isotope fractionation line that has a slope of ~0.5, as shown in Figure 1. Most equilibrium and kinetic isotope effects alter the abundances of ^{17}O and ^{18}O relative to ^{16}O (when measured relative to the isotope ratios in a standard material) in a 'mass-dependent' manner [7], so that $\lambda = 0.50$ to 0.529 in Eq. (1).[1]

$$\ln^{17}O = \lambda \times \ln^{18}O \quad (1)$$

A value for λ close to 0.5 is expected since isotope effects commonly scale with molecular velocities or vibrational energies, and these scale to good approximation (via the ratios of partition functions for the various isotopic species) with the mass differences between ^{16}O, ^{17}O, and ^{18}O, or simply (17–16)/(18–16) = 0.5 [11–14]. The value for λ in Eq. (1) for ozone in the atmosphere and laboratory, however, is far from 0.5, ranging from 0.65 to 1.0 [2,4–6,

[1] In this Letter, we report isotopic compositions in logarithmic notation for which the ^{18}O isotopic composition is given by $\ln^{18}O = \ln\left[\frac{(^{18}O/^{16}O)_{sample}}{(^{18}O/^{16}O)_{standard}}\right] = \ln[\delta^{18}O + 1]$ where $(^{18}O/^{16}O)_i$ is the ratio of the number of atoms of ^{18}O to ^{16}O in a sample or standard and $\delta^{18}O = \left[\frac{(^{18}O/^{16}O)_{sample}}{(^{18}O/^{16}O)_{standard}} - 1\right]$, and similarly for $\ln^{17}O$ and $\delta^{17}O$ [85]. Both the logarithmic and the delta notations for isotope compositions derive from isotope ratio mass spectrometry, in which the ratio of the rare to the common isotope is measured relative to that same ratio in a standard, as indicated in the definitions above. Because the ratio of two ratios can be measured with great precision, small but significant variations in the relative abundances of ^{16}O, ^{17}O, and ^{18}O resulting from physical, chemical, and biological isotope effects can be determined, even at the trace levels at which ^{17}O and ^{18}O occur naturally (^{16}O = 99.757%, ^{17}O = 0.038%, ^{18}O = 0.205%). While δ notation has been more commonly used to report isotopic compositions, we use the logarithmic notation to avoid curvature in the three isotope plots given the large range in isotopic compositions reported here. See Miller [8], Assonov and Brenninkmeijer [9], Coplen [10], and Luz and Barkan [85] for further details on isotope abundance reporting conventions and relationships, especially with regard to heavy oxygen isotope systematics.

* Corresponding author. Address: Department of Chemistry, Latimer Hall, UC Berkeley, Berkeley, CA 94720-1460, USA. Fax: +1 510 642 8369.
E-mail address: boering@berkeley.edu (K.A. Boering).

0009-2614/$ - see front matter © 2012 Elsevier B.V. All rights reserved.
http://dx.doi.org/10.1016/j.cplett.2012.10.038

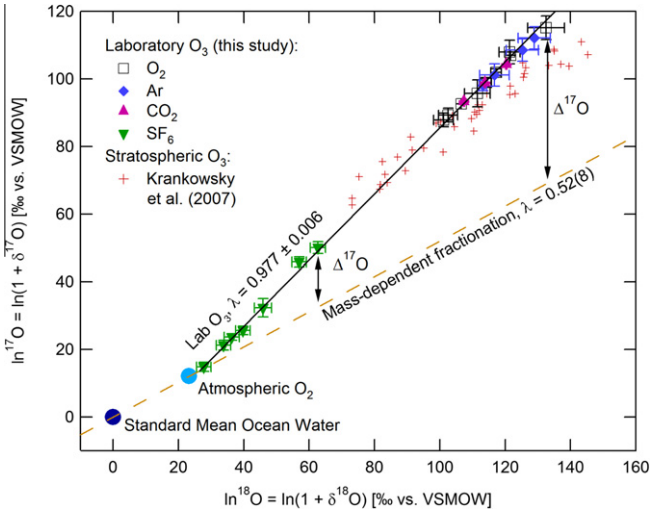

Figure 1. A 'three isotope plot' of the ^{17}O and ^{18}O isotopic compositions (measured relative to ^{16}O by definition)[1] of ozone, atmospheric O_2, and a reference standard (Vienna Standard Mean Ocean Water, or VSMOW). Most physical, chemical, and biological processes fractionate the isotopes of oxygen in a 'mass-dependent' manner – that is, the relative isotope enrichments or depletions for a process (measured relative to a standard) usually follow the relative mass differences between ^{16}O, ^{17}O, and ^{18}O. Therefore, most variations in the relative abundances of ^{16}O, ^{17}O, and ^{18}O measured relative to a standard will fall on the mass-dependent fractionation line shown in the figure (dashed brown line) with slope, λ, in Eq. (1) equal to ~0.5 (see text). Ozone, however, exhibits isotopic compositions that are distinctly 'non-mass-dependent' (also known as 'mass-independent' and 'anomalous'). Laboratory ozone measurements fall on a line with a slope very close to 1 (e.g., measurements from this study are plotted here along with results from a bivariate linear least squares regression with 2σ error given), while atmospheric ozone measurements exhibit a $\ln^{17}O/\ln^{18}O$ relationship of 0.65–1, depending on, e.g., temperature, pressure, and photolysis rates (with the most recent measurements for stratospheric ozone shown here [18]). Referring to isotopic compositions that fall off the mass-dependent line (and their underlying isotope fractionation process(es)) as 'non-mass-dependent' is more general than 'mass-independent' (since 'mass independent' implies that $\lambda = 1$). A useful measure of 'non-mass-dependence' is given by the quantity $\Delta^{17}O$, sometimes called the '^{17}O anomaly,' where $\Delta^{17}O = \ln^{17}O - \lambda_{MD} \ln^{18}O$ and λ_{MD} is a value for the mass-dependent slope that is very close to 0.5 but which can range from 0.50 to 0.053 depending on the processes or systems of interest [8,9,85]. $\Delta^{17}O$ represents the deviation of a $\ln^{17}O$ measurement from the mass-dependent fractionation line, as indicated by arrows in the figure.

15–21], depending on temperature, pressure, and other reactions that may be occurring in the vessel or environment; the most recently reported stratospheric ozone isotope measurements [18] are shown in Figure 1 as an example. Furthermore, statistical reaction rate theory applied to the ozone formation reaction [22,23] predicts that there should be small, mass-dependent *depletions* in ^{17}O and ^{18}O relative to ^{16}O, rather than the large, non-mass-dependent *enrichments* observed. Thus, statistical reaction rate theory errs in magnitude, three-isotope character, and sign.

Since the discovery of the unusual enrichments in ozone, experiments carried out by a number of research groups have led to the enrichments being attributed to isotope effects that arise in the ozone recombination reaction (2), with all reactants in their electronic ground states [20,24–27]:

$$O(^3P) + O_2(^3\textstyle\sum g^-) + M \rightarrow O_3^* + M \rightarrow O_3 + M^{\#} \quad (2)$$

The O_3^* complex is formed above the dissociation threshold and energy must be transferred to a third body, M, to form stable O_3. Given the nearly equal $\ln^{17}O$ and $\ln^{18}O$ enrichments (i.e., with λ near 1 in Eq. (1)), Thiemens and co-workers [4–6] first suggested that nuclear symmetry might play a role (since, e.g., $^{16}O^{16}O^{16}O$ has C_{2v} symmetry, while $^{17}O^{16}O^{16}O$ and $^{18}O^{16}O^{16}O$ are asymmetric and in the C_s point group). But a symmetry effect above and beyond the reduction in the densities of states of symmetric species that is already accounted for in statistical theories by the symmetry number is required, and earlier theories of symmetry-induced isotope effects [28–32] require the participation of electronically-excited states and/or their relevance to ozone formation has, at least for the time being, been discounted [33,34].

In 1999, Mauersberger and co-workers [35] published the first of a series of measurements of the isotope-specific rate coefficients for formation of a number O_3 isotopologues and isotopomers relative to the rate coefficient for formation of $^{16}O^{16}O^{16}O$, providing a critical step forward in advancing an understanding of the chemical physics of the unusual isotope enrichments. These were also surprising in that (1) the rate coefficient enhancements were as large as 52% (for $^{16}O + {}^{18}O^{18}O \rightarrow {}^{16}O^{18}O^{18}O$); (2) symmetry alone was not a controlling factor in the rate coefficient enhancements for individual isotope-specific ozone formation channels (since, e.g., formation of the asymmetric species $^{18}O^{16}O^{16}O$ by $^{18}O + {}^{16}O^{16}O$ was actually slower than formation of $^{16}O^{16}O^{16}O$); and (3) the rate coefficient enhancements for the asymmetric species were found to roughly scale with the very small zero-point energy differences of ~10–20 cm^{-1} between the isotopologues [36] and, thus, in turn, with the relative mass differences and hence were 'mass-dependent'. When these new data were combined with the earlier enrichment studies [19,20,24], Marcus and co-workers [37–41], in a modified RRKM treatment, showed that all the experimental results under a variety of conditions could be explained by a combination of two isotope effects.

The first isotope effect Marcus and co-workers [38,39,41] suggested is a very large mass-dependent isotope effect (called the 'ΔZPE effect'), which depends sensitively on the small zero-point energy differences (ΔZPE) between the two O_2 isotopologues from which a particular asymmetric ozone can be formed. For example, $^{18}O^{16}O^{16}O$ can be formed from either $^{16}O^{16}O$ reacting with ^{18}O or $^{18}O^{16}O$ reacting with ^{16}O, so ΔZPE refers to the difference in zero point energies between $^{16}O^{16}O$ and $^{18}O^{16}O$. This effect cancels out when ozone can be formed from both (or all) O_2 pathways (i.e., under the 'scrambled' O_2 isotopologue conditions in the atmosphere and most laboratory conditions). A number of theoretical studies, including quantum [42–45] and semi-classical [34,46,47] calculations, have provided additional physical insight into this first isotope effect and confirm the important role that ΔZPE plays under 'unscrambled' conditions.

The second isotope effect first suggested by Marcus and co-workers [38,39,41] – and the one that is responsible for the large, non-mass-dependent isotope enrichments in ozone formed in the atmosphere and under most laboratory conditions – has been called the 'η effect.' Its origin remains unexplained. Marcus and co-workers [38,39,41] calculated it empirically within their RRKM framework by fitting the fastest and the slowest isotope-specific ozone formation rate coefficients measured by Mauersberger and co-workers [33,35,36,48–51] and showed that the effective density of states of O_3^* in an RRKM treatment – and therefore the recombination rate coefficient for $O + O_2$ – must be 18% lower for symmetric ozone than for asymmetric ozone isotopomers. They suggested that this *ad hoc* η effect could arise, for example, from the absence of some of the anharmonic vibration–vibration coupling and Coriolis rotational-vibrational coupling terms for symmetric O_3^* so that the effective density of states that couple to the exit channel is smaller for symmetric O_3^* than for asymmetric O_3^*, thus lowering the relative rate coefficient even further from the statistical prediction than for asymmetric O_3 [38,52]. Similarly – but using quasi-classical trajectory calculations – Schinke and co-workers [34,46] also found that their treatment required an *ad hoc* means of enhancing the formation rate coefficients for the asymmetric ozone species relative to the symmetric species of the same order of magnitude (15%) as that of Marcus et al. Based on these and other theoretical results [32,53–62], it has thus been suggested

that the 'η effect' is some sort of a dynamically-driven quantum symmetry effect that affects the lifetimes of the excited ozone complexes (e.g., via bottlenecks in intramolecular energy redistribution) and/or the efficiency of their collisional stabilization (e.g., via bottlenecks in intermolecular energy redistribution) of the symmetric and asymmetric O_3^* complexes differently. Recently both Schinke et al. [57,63] and Marcus et al. [60–62] have suggested that the η effect might arise from the slow, Coriolis-driven diffusion of the K-component of the total angular momentum J of the near symmetric top O_3^* during collisions and/or the time between collisions and that, furthermore, there may be an isotopic symmetry dependence to the coupling; these differences could then lead to non-RRKM effects whose magnitudes would depend on molecular symmetry. Despite these promising ideas, however, calculations to date of this slow K-component diffusion do not yet show the required isotopic symmetry dependence, and so the η effect remains unexplained.

In short, although fascinating new insights into unusual kinetic isotope effects in the 3-body ozone formation reaction have been gained over the past decade through a variety of sophisticated experimental and computational efforts, the chemical physics underlying the η effect remains unresolved. Basic questions remain, including the nature and origin of the symmetry effect itself and whether it affects the relative isotope-specific O_3^* lifetimes prior to collisional stabilization, the collisional stabilization step, or both. Indeed, even the relative contributions of the 'energy transfer' (ET) mechanism (e.g., $O + O_2 \leftrightarrow O_3^*$ followed by $O_3^* + M \rightarrow O_3$ shown in Eq. (2)) versus the 'chaperone' or 'radical complex' (RC) mechanism (e.g., $O_2 + M \leftrightarrow O_2 \cdot\cdot M$ followed by $O_2 \cdot\cdot M + O \rightarrow O_3 + M$) to the formation of ozone at typical atmospheric and laboratory conditions, as well as the consequences of isotopic substitution for the ET or RC mechanisms on the isotope-specific formation rate coefficients, are still in question [34,64–68].

To gain further insight into the chemical physics of the η effect in ozone formation and to provide new benchmarks for theory, we have measured the pressure and bath gas dependence of the ^{17}O and ^{18}O enrichments in ozone formed in the laboratory by photolysis of O_2 under 'scrambled' conditions, studying a range of bath gases with very different quenching efficiencies for ozone formation: Ar, O_2, CO_2 and SF_6. To date, few experiments measuring the isotopic composition of O_3 formed in the presence of different bath gases have been performed [6,49,69–71], and none with bath gases beyond the complexity of CO_2. Moreover, all previous bath gas experiments were performed prior to the insights into the chemical physics of the problem that have been gained from the various theoretical studies over the last decade cited above; thus, new insight into the η effect can be gained from comparing the experimental results presented here with expectations based on current understanding.

2. Methods

Ozone was produced in the apparatus shown in Figure 2 by photolysis of O_2 at 184.9 nm in a 2.2 liter borosilicate glass bulb equipped with a low-pressure mercury/argon pen lamp (Oriel Instruments). After steady-state ozone concentrations were reached, (30–120 min), the ozone was collected and separated cryogenically from the various bath gases and then analyzed by dual inlet, viscous flow isotope ratio mass spectrometry (IRMS).

The apparatus was first pre-conditioned with O_3 in order to remove impurities that react with ozone. Then, in each of the experiments, O_2 gas (Scott Specialty Gases, 99.999%) was introduced into the bulb to a pressure of 50 Torr (or higher for the experiments using O_2 as the bath gas), as measured by an absolute pressure transducer (MKS Baratron model 697B10, 1000 Torr full-scale, 0.1% accuracy). The initial isotopic composition of O_2 in the bulb was $\ln^{17}O = 13.7 \pm 0.2‰$ (2σ) and $\ln^{18}O = 26.5 \pm 0.2‰$ (2σ) relative to the VSMOW international isotope standard, based on 3 separate control runs without irradiation. Following introduction of O_2 into the photolysis bulb, the bath gases Ar (Praxair, 99.999%), CO_2 (Scott Specialty Gases, 99.999%), or SF_6 (Sigma–Aldrich, 99.95%) were added, with CO_2 and SF_6 receiving additional purification before addition to the bulb by several freeze–pump-thaw cycles. A photochemical model [72] shows that ozone reaches a steady-state in isotopic composition after 1 min and a steady-state in concentration after 30 min–2 h (depending on the total pressure and bath gas) after the start of irradiation. These times are upper limits since the J-values for O_2 and O_3 photolysis used in the model were estimated based on the geometry of the bulb and the lower limit of the photon flux (4.3×10^{13} cm^{-2} s^{-1}) of the mercury lamp at 184.9 nm that was determined by CO_2 actinometry. Experiments carried out to longer irradiation times showed no change in isotopic composition, confirming that isotopic steady state was reached. We also note that, although the CO_2 bath gas can exchange oxygen isotopes with ozone [73–75], significant isotope exchange occurs on time scales of many hours under our experimental conditions. On the

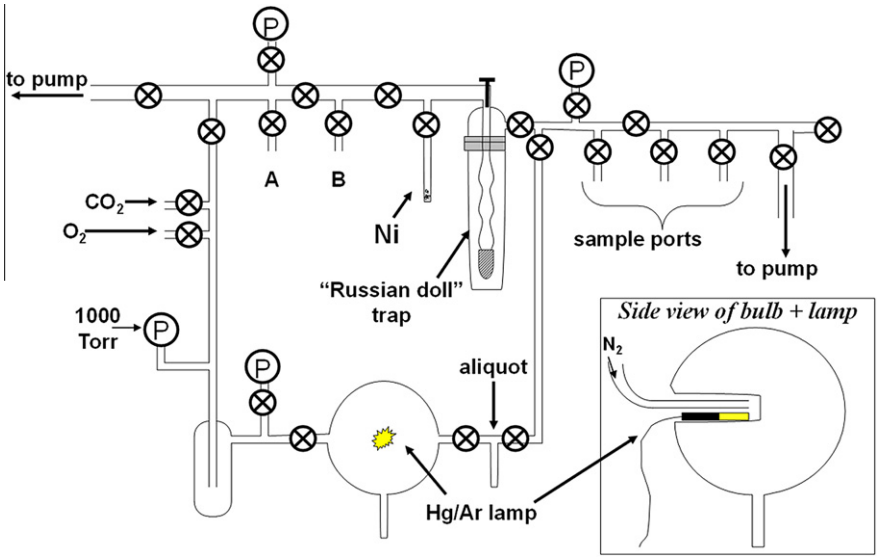

Figure 2. Schematic of the bulk photochemical apparatus for production of ozone from photolysis of O_2 as a function of the pressure of Ar, O_2, CO_2, and SF_6.

30-min irradiation time scale of the CO_2 bath gas experiments, our photochemical model predicts that the extent of isotope exchange between CO_2 and ozone is negligible, affecting CO_2 and O_3 to less than <0.7‰. These model predictions were confirmed by a 30-min irradiation experiment with 50 Torr of O_2 and 125 Torr of CO_2 in which the isotopic composition of CO_2 changed by only +0.1‰ for $\ln^{17}O$ and +0.2‰ for $\ln^{18}O$, which is within the 2σ uncertainty of the isotopic reproducibility of the control experiments without irradiation.

After irradiation, O_3 was collected and separated from the remaining O_2 and any bath gases in the photolysis bulb by multi-step cryogenic separation. Ozone was separated from Ar and O_2 by collecting the ozone at liquid nitrogen temperature (−196 °C) in a cold trap and pumping away the remaining O_2 and Ar. For the CO_2 and SF_6 experiments, ozone and either CO_2 or SF_6 were collected in a Russian doll trap [76] followed by several additional cryogenic separation steps in fingers at ports A and B at liquid N_2 and ethanol slurry (−100 °C) temperatures; see Figure 2. The bath gases were pumped away at a sufficiently rapid rate so as to avoid isotopic fractionation due to evaporation of O_3, which has a vapor pressure of 0.7 mTorr at −196 °C [77,78]. The collected ozone was then cryogenically transferred to a sample tube in which it was catalytically converted to O_2 on nickel by heating to ~60 °C for 10–15 min. The amount of O_2 produced from the decomposition of ozone was determined manometrically in a calibrated volume and ranged from 15 to 50 μmol depending on bath gas, pressure, and irradiation time (e.g., if irradiation was ceased before the ozone steady-state concentration was reached in a particular run). The O_2 was then transferred to a sample tube containing 13× molecular sieve (Sigma–Aldrich) held at liquid nitrogen temperature. For the CO_2 and SF_6 experiments, a gas chromatograph was also used to further purify the O_2 obtained from O_3 decomposition prior to IRMS analysis (GOW-MAC Series 400 GC with a 4 m × 1/8″ molecular sieve 5A column [45/60 mesh], helium backing pressure and flow rate of 38 psig and 30 mL/min, respectively, and a thermal conductivity detector). This additional step was particularly important for O_2 from the SF_6 experiments since trace amounts of SF_6 can produce NF^+ ions (m/z 33) from ion–molecule reactions with background N_2 in the ion source, producing an isobaric interference with $^{17}O^{16}O$ and thus positive artifacts in $\Delta^{17}O$ values (see Figure 1 for an illustration and definition of $\Delta^{17}O$).

After purification, each resulting O_2 sample from O_3 decomposition was immediately analyzed on a dual inlet Finnigan MAT 252 IRMS for the ^{17}O and ^{18}O isotopic compositions. The single measurement precisions for $\ln^{17}O$ and $\ln^{18}O$ of O_2 were typically ±0.05‰ and ±0.03‰ (2σ), respectively. The resulting $\ln^{17}O$, $\ln^{18}O$, and $\Delta^{17}O$ values are given in Table 1. The 2σ uncertainties for $N > 1$ range from ±1.0 to ±4.0‰ for $\ln^{17}O$, from ±1.1 to ±5.6‰ for $\ln^{18}O$, and from ±0.5 to ±4.1‰ for $\Delta^{17}O$. Mass-dependent fractionation resulting from small losses during O_3 and O_2 purification is a possible source of random and systematic error and is likely the main contributor to the 2σ uncertainties. This is consistent with the fact that the $\Delta^{17}O$ uncertainties are typically somewhat smaller than those for $\ln^{17}O$ and $\ln^{18}O$ since small degrees of mass-dependent fractionation due to sample handling cancel out for $\Delta^{17}O$ by definition [9]. Mass-dependent fractionation due to inefficiencies in O_3 collection, however, does not appear to be large since our results for an O_2 bath gas are consistent with the previous measurements of Morton et al. [20], who trapped the ozone produced in their experiment at −208 °C, at which the vapor pressure of ozone is a factor of 70 lower (0.01 mTorr) than that at −196 °C in our experiments. This suggests that the purification of O_2 from the different bath gases may play a larger role in determining the precision of the results than O_3 losses during cryogenic separation. Other possible contributors to the 2σ uncertainties, as well as the overall uncertainty in isotopic compositions, include (1) potential variations in the lamp flux between different runs (which could induce mass-dependent fractionation directly by changing the rate of ozone photolysis or indirectly by changing the concentrations of $O(^1D)$, $O_2(^1\Delta)$, and $O_2(^1\Sigma)$ that have potentially significant mass-dependent kinetic isotope effects in reactions with O_3 [72]) or (2) mean temperature differences in the bulb between runs due to potential variations in the lamp flux or laboratory conditions between runs (which could alter $\ln^{17}O$, $\ln^{18}O$, and possibly $\Delta^{17}O$ due to the

Table 1
The isotopic composition of ozone formed by irradiation of O_2 at 50 Torr of O_2 or higher or by irradiation of O_2-bath gas mixtures consisting of 50 Torr of O_2 and (P – 50 Torr) of bath gas. Values for $\ln^{17}O$ and $\ln^{18}O$ are given relative to the starting isotopic composition of O_2 and expressed as per mil (‰). A value for λ_{MD} of 0.52 is used to calculate $\Delta^{17}O$ where $\Delta^{17}O = \ln^{17}O - \lambda_{MD}\ln^{18}O$ (see Figure 1 caption). Errors given are for the 95% confidence intervals (1.96σ); N is the number of runs at each pressure.

Bath Gas	P (Torr)	$\ln^{17}O$ (‰)	$\ln^{18}O$ (‰)	$\Delta^{17}O$ (‰)	Slope	N
O_2	50	101.5 ± 3.5	106.0 ± 5.6	46.3 ± 1.7	0.96	4
O_2	100	94.3 ± 3.5	94.9 ± 3.2	44.9 ± 2.6	0.99	4
O_2	175	93.3 ± 0.08	95.1 ± 0.05	43.8 ± 0.11	0.98	2
O_2	300	88.3 ± 1.1	90.7 ± 1.6	41.1 ± 0.5	0.97	4
O_2	400	85.3 ± 1.3	87.5 ± 1.8	39.7 ± 2.2	0.97	2
O_2	500	82.0 ± 4.0	84.9 ± 3.9	37.9 ± 2.2	0.97	4
O_2	600	78.9 ± 0.02	80.1 ± 0.04	37.30 ± 0.08	0.99	1
O_2	700	75.6 ± 2.1	76.0 ± 2.9	36.1 ± 1.3	0.99	4
O_2	760	74.1 ± 2.0	74.6 ± 3.0	35.3 ± 3.6	0.99	4
				Average Slope	*0.98*	*±0.03*
Ar	100	98.4 ± 3.3	102.4 ± 4.9	45.2 ± 2.1	0.96	4
Ar	300	94.8 ± 3.4	98.7 ± 5.0	43.5 ± 2.3	0.96	3
Ar	500	87.5 ± 3.3	90.2 ± 4.5	40.6 ± 0.9	0.97	4
Ar	700	84.3 ± 1.6	86.7 ± 1.1	39.2 ± 1.2	0.97	4
				Average Slope	*0.97*	*±0.01*
CO_2	175	90.6 ± 0.05	93.9 ± 0.09	41.75 ± 0.08	0.96	1
CO_2	300	85.1 ± 0.05	87.3 ± 0.05	39.71 ± 0.06	0.97	1
CO_2	500	79.6 ± 0.04	80.9 ± 0.04	37.52 ± 0.05	0.98	1
				Average Slope	*0.97*	*±0.02*
SF_6	100	36.4 ± 1.7	36.2 ± 2.3	17.5 ± 2.3	1.00	2
SF_6	175	32.2 ± 1.5	30.4 ± 2.2	16.4 ± 2.7	1.06	3
SF_6	300	18.7 ± 2.7	19.3 ± 2.6	8.6 ± 4	0.97	2
SF_6	400	11.9 ± 1.3	13.3 ± 2.2	5.1 ± 2.4	0.90	2
SF_6	500	10.0 ± 1.0	9.8 ± 2.4	4.9 ± 2.2	1.02	2
SF_6	600	7.6 ± 1.5	7.3 ± 2.3	3.8 ± 2.7	1.04	2
SF_6	700	1.2 ± 1.4	1.2 ± 2.2	0.5 ± 0.2	0.95	2
				Average Slope	*0.99*	*±0.11*

temperature dependence of these quantities in ozone formation [18,51,79]). A variation of ±2.5 °C in bulb temperature, for example, would yield differences in isotopic compositions of ±0.6‰, ±0.75‰, and ±0.20‰ for $\ln^{17}O$, $\ln^{18}O$, and $\Delta^{17}O$, respectively. Overall, these uncertainties are small compared to the very large heavy isotope enrichments in ozone we measure and to the sensitivity of those enrichments to the identity of the bath gas that we report below.

For comparison with experimental results, we used a photochemical kinetics model to predict the steady-state ozone isotopic compositions for O_2. The basic model is described in detail in Cole and Boering [72] and is run in KINTECUS software (J.C. Ianni, Kintecus, Windows Version 3.962, www.kintecus.com [80]). The model includes two types of isotope effects: the very fast isotope exchange between O and O_2 [22,23,72,81] and the isotope-specific rate coefficients measured by Mauersberger and co-workers [33,35,36,48–51] or derived from them; see Cole and Boering [72] for details. This model successfully predicts the isotopic enrichment for O_3 at 50 Torr, and to within the uncertainty of possible isotope effects in the photolysis of O_3. For example, incorporating the (mass-dependent) photolyis isotope effects for ozone at 254 nm calculated by Liang et al. [82] into the model produces ozone with values for $\ln^{17}O$ and $\ln^{18}O$ that are 3‰ and 6‰ lower, respectively, than values from the model runs that do not include photolysis isotope effects at 254 nm.

For comparison with the pressure- and bath gas-dependent results presented here, we multiplied the rate coefficient for formation of $^{16}O^{16}O^{16}O$ from collisions of O_3^* with Ar, CO_2, or SF_6 in the model by the experimentally-determined, room-temperature quenching efficiencies of 0.7, 2.1, and 5.3 for the formation of $^{16}O^{16}O^{16}O$ [64,66]. In addition, an empirical pressure dependence for the isotope-specific KIEs of Mauersberger and co-workers in an O_2 bath gas was derived from our data for the ozone isotope enrichment data in O_2 bath gas assuming that all the pressure dependence is carried by the rate coefficients for the asymmetric formation channels $^{16}O + {}^{18}O^{16}O$ and $^{16}O + {}^{17}O^{16}O$. This assumption is in line with expectations from experimental data [49] and theoretical treatments [41] at the pressures of this study, as well as with previous experimental results for the isotope enrichments in scrambled mixtures. The modified model provides a guide for what order of magnitude of isotope enrichments would be expected in ozone if the relative quenching efficiencies for formation of $^{16}O^{16}O^{16}O$ were the only physical process relevant for formation of the other isotopologues of ozone in the different bath gases. We know this is not the case, since, for example, the ozone isotope enrichments in an O_2 bath gas decrease significantly with increasing pressure above 1 bar and disappear at 56 bar [19], while the fall-off region for the rate coefficient for formation of $^{16}O^{16}O^{16}O$ is not reached until significantly higher pressures [64,66]. Nevertheless, the relative agreement and disagreement of the simple model predictions with experimental results for the different bath gases provides some phenomenological insight into the bath-gas dependence of the ozone isotope enrichments based on relative quenching efficiencies alone, as we describe below.

3. Results and discussion

Results for the ^{17}O and ^{18}O enrichments in ozone as a function of pressure and bath gas from 50 to 760 Torr total pressure are shown in Figures 1 and 3 and given in Table 1. For the O_2 experiments, the values are very similar to those measured previously [19,20] (also shown in Figure 3), to an empirical expression for the pressure dependence of the ^{18}O enrichments in O_2 bath gas [49], and to several measurements in an 80% N_2/20% O_2 bath gas [20]. While $\ln^{17}O$, $\ln^{18}O$, and $\Delta^{17}O$ all decrease with pressure (Figure 3), the ratio of

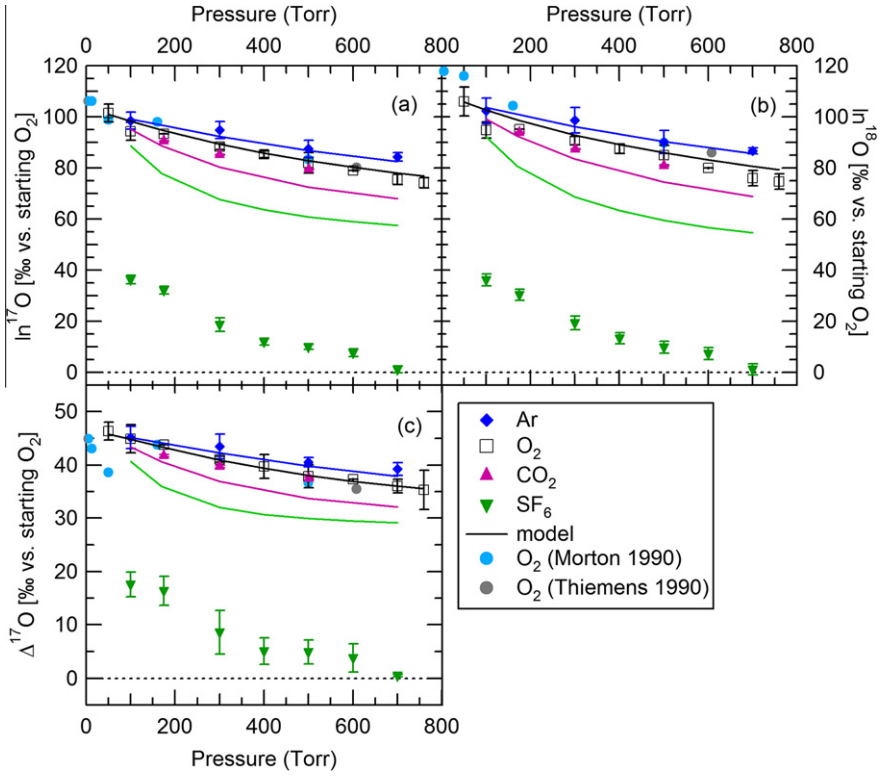

Figure 3. Measured ozone isotope enrichments (non-circular symbols) as a function of pressure for (a) $\ln^{17}O$ (b) $\ln^{18}O$ and (c) $\Delta^{17}O = \ln^{17}O - 0.52\ln^{18}O$ expressed as ‰ ('per mil') relative to the starting O_2 isotopic composition (dashed line). Also shown are experimental results from Morton et al. [20] and Thiemens and Jackson [19] (circles). Predictions from a photochemical kinetics model (lines, color-coded by bath gas) are also shown for comparison (see Section 2). (Note that the deviations in $\Delta^{17}O$ in the previous studies for pressures <50 Torr from the trends measured in all the O_2 bath gas studies at higher pressures are most likely due to the increasing importance of ozone formation on walls, which does not exhibit the anomalous isotope effects associated with ozone recombination in the gas phase [86]).

$\ln^{17}O$ to $\ln^{18}O$ (i.e., the value for λ in Eq. (1)) relative to the starting O_2 isotopic composition is quite constant at 0.977 ± 0.006 (2σ) overall (Figure 1). Notably, there are significant differences in the ozone isotopic composition between bath gases for a given total pressure (at the 1σ or greater level in most instances), and the enrichments follow the order Ar > O_2 > CO_2 > SF_6. This order follows the values for the average amount of energy transferred per collision (ΔE) of 18, 25, 150 and 280 cm^{-1}, respectively (assuming O_2 is similar to N_2), which were derived from non-isotope-specific kinetics studies of ozone formation [66]. The larger the ΔE for ozone formation, the smaller the ozone enrichments for a given collision frequency, as predicted by Gao and Marcus [41]. Interestingly, however, the measured ozone enrichments for the O_2 and CO_2 bath gases are quite similar in magnitude for a given pressure, despite the larger number of internal degrees of freedom and the factor of ~2 larger quenching efficiency and factor of ~6 larger ΔE for forming $^{16}O^{16}O^{16}O$ for CO_2 than for O_2. In contrast, the ozone enrichments with SF_6 as the bath gas are dramatically lower than for O_2 and CO_2 at all pressures measured. Indeed, the isotope selectivity of ozone formation in an SF_6 bath gas has been eliminated (to within experimental error) by 700 Torr total pressure. In contrast, for ozone formation in an O_2 bath gas, a pressure of 56 bar is required before the isotopic enrichments disappear [19].

The small difference between the CO_2 and O_2 bath gas results for a given total pressure and the very large difference between the SF_6 and CO_2 bath gas results in Figure 3 suggest that we can use different bath gases to probe the region of the potential energy surface for O_3^* that is most sensitive to the η effect – that is, the most sensitive to the differences between the asymmetric and symmetric O_3^* complexes with respect to their lifetimes and/or collisional stabilization probabilities. A value for ΔE of ~280 cm^{-1} (i.e., for SF_6) is dramatically more effective at diminishing the influence of the η effect than a ΔE of ~150 cm^{-1} (i.e., for CO_2), even at very low pressures (i.e., collision frequencies), suggesting we are probing with these two different bath gases a threshold regime on the PES where the η effect is most relevant and effective at producing anomalous enrichments in the ozone formed.

This departure of the experimental results from expectations based simply on ΔE values derived from non-isotope specific ozone formation studies is phenomenologically evident from the model predictions shown as lines in Figure 3. For example, if the relative quenching efficiencies to form ozone derived from the non-isotope-specific studies were solely responsible for determining the isotopic enrichments in ozone formed in the experiments, then ozone formed in the CO_2 bath gas would be significantly less enriched (magenta line) than measured (magenta symbols), and ozone formed in the SF_6 bath gas (green line) would be much more enriched than measured (green symbols). Importantly, experimental artifacts (e.g., isotope exchange with ozone for CO_2 bath gas and an NF^+ isobaric interference for SF_6 bath gas), if present at all, would cause the enrichments to go in the opposite directions than those discussed here (see Section 2). The SF_6 measurements compared with the CO_2 and O_2 results thus suggest that a value for ΔE as large as 280 cm^{-1}, or some other important characteristic(s) of energy transfer between SF_6 and O_3^*, allows O_3^* to more efficiently bypass the most isotope selective region of the O_3^* PES, while a value of ΔE of ~150 cm^{-1} or less, or some other characteristic(s) of energy transfer between CO_2 and O_3^*, does not. Experiments with additional bath gases with masses and degrees of freedom intermediate between those of CO_2 and SF_6, such as CF_4, are planned to further test this idea of a ΔE probe of the η effect.

Alternatively, it is conceivable that the experimental results are suggestive of a difference between SF_6 and the other bath gases in the relative contributions of the radical complex (RC) mechanism versus the energy transfer (ET) mechanisms in ozone formation. For example, analysis of non-isotope-specific kinetics data by Troe and co-workers [66] suggests that 40% of ozone formation occurs via the RC and 60% via the ET mechanism at room temperature and low pressures for the bath gases Ar and N_2, with an increasing contribution of RC at lower temperatures and higher pressures. If the unusual kinetic isotope effects in ozone formation are associated only with the ET mechanism, as has been conjectured before [64,71], then a larger contribution from the RC mechanism for SF_6 as bath gas might lower even further the anomalous enrichments in ozone expected from the ET mechanism alone, relative to the other bath gases studied. Indeed, a change in the relative contributions of the RC versus ET mechanisms may be one explanation for the observed decrease in anomalous ozone enrichments as temperature decreases [51,68,79]. For the case of the bath gas differences, if the $M\cdot\cdot O_2$ and/or $M\cdot\cdot O$ complexes are more stable for M = SF_6 than for M = O_2, CO_2, and Ar and at the same time are more likely to result in a stabilized O_3, then it is possible that at least part of the dramatic decrease in the ozone enrichments we measure in SF_6 bath gas could be attributed to an increased role for the RC mechanism. Kinetics data to date on formation of $^{16}O^{16}O^{16}O$ in SF_6 and CO_2 are still too inconclusive [66] to estimate the parameters needed and to extrapolate to what might be expected for the magnitude of such an effect on the ozone enrichments. However, similar experiments to those reported here performed as a function of temperature below room temperature could shed light on the extent to which the RC mechanism may be diminishing the influence of the η effect in the experiments and provide additional benchmarks for theory.

Finally, we note that previous experimental results for the bath gas dependence of the ratios of the relative formation rate coefficients for $^{16}O + {}^{18}O^{18}O/{}^{16}O + {}^{16}O^{16}O$ and for $^{18}O + {}^{16}O^{16}O/{}^{18}O + {}^{18}O^{18}O$ have been interpreted to mean that there is no dependence of the ozone isotope effects on bath gas identity [49,71]. In turn, this has been interpreted to mean that (1) the isotope enrichments must result from O_3^* formation or dissociation and not collisional stabilization [71] and that (2) various theoretical treatments can be performed for a collision partner such as Ar and the results would be generalizable to all bath gases [83,84]. Our results here suggest that these interpretations are oversimplifying the processes involved and that bath gas identity is an important consideration. First, the Guenther et al. [71] experiments were for formation of ozone in 'unscrambled' experiments; thus, they were largely probing the sensitivity of the ΔZPE isotope effect to bath gas identity and not the η effect. Second, the most complex bath gas Guenther et al. [71] explored was CO_2, and our results for the bath gas dependence of the η effect show that CO_2 as a bath gas was not dramatically different from O_2 as a bath gas. Indeed, Gao and Marcus' treatment [41] of the pressure dependence of the ratio of isotope-specific rate coefficients in the unscrambled experiments of Guenther et al. [49] shows that a dependence on bath gas identity (via ΔE) is expected, in addition to a pressure dependence, albeit a dependence that may require a much larger ΔE than probed with CH_4 and CO_2 by Guenther et al. or higher pressures than were experimentally feasible. Our results here, combined with the predictions of Gao and Marcus [41], therefore suggest that it is important to repeat the rate coefficient ratio experiments of Guenther et al. using SF_6 as the bath gas, which may reveal a bath gas dependence to the rate coefficient ratios for ozone formation and at pressures more easily accessible than in the previous 'unscrambled' experiments in noble gas, O_2, CH_4, and CO_2 bath gases.

4. Conclusions

Measurements of the bath gas and pressure dependence of the heavy isotope enrichments in ozone formed by photolysis of O_2 in the presence of Ar, O_2, CO_2, and SF_6 from 50 to 760 Torr show a de-

crease in $\ln^{17}O$, $\ln^{18}O$, and $\Delta^{17}O$ with increasing pressure and with increasing quenching efficiency of the bath gas. The decrease in enrichments with SF_6 as bath gas are particularly dramatic. Indeed, for SF_6 all isotope selectivity to form ozone is eliminated (to within experimental error) at the relatively low total pressure of 700 Torr, and thus confirms the importance of both ΔE and collision frequency in determining the magnitude of the influence of the η effect on ozone isotopic compositions under the common 'scrambled' conditions in the atmosphere and most laboratory experiments, as predicted by Gao and Marcus [41]. The large difference between the results for SF_6 bath gas and other gases, combined with the similarity of enrichments for O_2 and CO_2, suggest a 'threshold' ΔE for which the influence of the η effect is greatly diminished, other bath gas characteristics that may provide significantly more facile energy transfer between SF_6 and O_3^* than for CO_2 and O_2 with O_3^*, and/or a larger relative contribution of the radical complex mechanism for SF_6 than for the other bath gases. Thus, these new results provide insights into the role that bath gas characteristics and energy transfer may play in the unusual ozone formation isotope effects under thermal conditions, as well as important new benchmarks for theoretical and computational studies of the nature and origin of the dynamically-driven, symmetry-related η effect in ozone formation and, in turn, the extent to which this unusual isotope effect may be generalizable to other chemical systems. Specifically, the bath gas and pressure dependence results presented here provide new constraints for detailed theoretical investigations into whether the η effect may be largely governed by bottlenecks in intramolecular energy redistribution in the O_3^* complex, by bottlenecks in intermolecular energy redistribution O_3^* and bath gas M, and/or to what extent a RC mechanism may also come into play in determining the unusual heavy isotope enrichments in ozone in the laboratory and atmosphere.

Acknowledgements

This material is based upon work supported by the US National Science Foundation under Grant No. CHE-0809973. The authors also gratefully acknowledge a Camille Dreyfus Teacher-Scholar Award (K.A.B), postdoctoral support (K.L.F.) from The Danish Council for Independent Research/Natural Sciences and the Carlsberg Foundation, and Carl Brenninkmeijer, Rudy Marcus, and anonymous reviewers for thoughtful comments and suggestions.

References

[1] K. Mauersberger, Geophys. Res. Lett. 8 (1981) 935.
[2] K. Mauersberger, Geophys. Res. Lett. 14 (1987) 80.
[3] K. Mauersberger, P. Lammerzahl, D. Krankowsky, Geophys. Res. Lett. 28 (2001) 3155.
[4] M.H. Thiemens, J.E. Heidenreich III, Science 219 (1983) 1073.
[5] J.E. Heidenreich III, M.H. Thiemens, J. Chem. Phys. 78 (1983) 892.
[6] J.E.I. Heidenreich, M.H. Thiemens, J. Chem. Phys. 84 (1986) 1986.
[7] M.H. Thiemens, Annu. Rev. Earth Planet. Sci. 34 (2006) 217.
[8] M.F. Miller, Geochim. Cosmochim. Acta 66 (2002) 1881.
[9] S.S. Assonov, C.A.M. Brenninkmeijer, Rapid Commun. Mass Spectrom. 19 (2005) 627.
[10] T.B. Coplen, Rapid Commun. Mass Spectrom. 25 (2011) 2538.
[11] H.C. Urey, J. Chem. Soc. (1947) 562.
[12] J. Bigeleisen, M. Goeppert Mayer, J. Chem. Phys. 15 (1947) 261.
[13] R.E. Weston, Chem. Rev. 99 (1999) 2115.
[14] R.E. Weston, J. Nucl. Sci. Technol. 43 (2006) 295.
[15] B. Schueler, J. Morton, K. Mauersberger, Geophys. Res. Lett. 17 (1990) 1295.
[16] D. Krankowsky, F. Bartecki, G.G. Klees, K. Mauersberger, K. Schellenbach, J. Stehr, Geophys. Res. Lett. 22 (1995) 1713.
[17] D. Krankowsky, P. Lammerzahl, K. Mauersberger, Geophys. Res. Lett. 27 (2000) 2593.
[18] D. Krankowsky, P. Lammerzahl, K. Mauersberger, C. Janssen, B. Tuzson, T. Rockmann, J. Geophys. Res. Atmos. 112 (2007) D08301.
[19] M.H. Thiemens, T. Jackson, Geophys. Res. Lett. 17 (1990) 717.
[20] J. Morton, J. Barnes, B. Schueler, K. Mauersberger, J. Geophys. Res. 95 (1990) 901.
[21] J.C. Johnston, M.H. Thiemens, J. Geophys. Res. Atmos. 102 (1997) 25395.
[22] J.A. Kaye, D.F. Strobel, J. Geophys. Res. 88 (1983) 8447.
[23] J.A. Kaye, J. Geophys. Res. 91 (1986) 7865.
[24] K. Mauersberger, J. Morton, B. Schueler, J. Stehr, S.M. Anderson, Geophys. Res. Lett. 20 (1993) 1031.
[25] D.W. Arnold, C.S. Xu, E.H. Kim, D.M. Neumark, J. Chem. Phys. 101 (1994) 912.
[26] S.M. Anderson, A.D. Hulsebusch, K. Mauersberger, J. Chem. Phys. 107 (1997) 5385.
[27] S.M. Anderson, K. Mauersberger, J. Geophys. Res. 100 (1995) 3033.
[28] J.J. Valentini, J. Chem. Phys. 86 (1987) 6757.
[29] P.L. Houston, A.G. Suits, R. Toumi, J. Geophys. Res. 101 (1996) 18.
[30] J.K. Xie, B. Poirier, G.I. Gellene, J. Am. Chem. Soc. 127 (2005) 16969.
[31] G.I. Gellene, Science 274 (1996) 1344.
[32] R.T. Pack, R.B. Walker, J. Chem. Phys. 121 (2004) 800.
[33] K. Mauersberger, D. Krankowsky, C. Janssen, R. Schinke, in: B. Bederson, H. Walther (Eds.), Advances in Atomic, Molecular, and Optical Physics, Elsevier Inc., 2005, p. 1.
[34] R. Schinke, S.Y. Grebenshchikov, M.V. Ivanov, P. Fleurat-Lessard, Annu. Rev. Phys. Chem. 57 (2006) 625.
[35] K. Mauersberger, B. Erbacher, D. Krankowsky, J. Gunther, R. Nickel, Science 283 (1999) 370.
[36] C. Janssen, J. Guenther, K. Mauersberger, D. Krankowsky, Phys. Chem. Chem. Phys. 3 (2001) 4718.
[37] B.C. Hathorn, R.A. Marcus, J. Chem. Phys. 111 (1999) 4087.
[38] Y.Q. Gao, R.A. Marcus, Science 293 (2001) 259.
[39] Y.Q. Gao, W.C. Chen, R.A. Marcus, J. Chem. Phys. 117 (2002) 1536.
[40] R.A. Marcus, J. Chem. Phys. 124 (2006).
[41] Y.Q. Gao, R.A. Marcus, J. Chem. Phys. 127 (2007) 244316.
[42] D. Babikov, B.K. Kendrick, R.B. Walker, R.T. Pack, P. Fleurat-Lesard, R. Schinke, J. Chem. Phys. 119 (2003) 2577.
[43] D. Babikov, B.K. Kendrick, R.B. Walker, R. Schinke, R.T. Pack, Chem. Phys. Lett. 372 (2003) 686.
[44] D. Babikov, B.K. Kendrick, R.B. Walker, R.T. Pack, P. Fleurat-Lesard, R. Schinke, J. Chem. Phys. 118 (2003) 6298.
[45] S.Y. Grebenshchikov, R. Schinke, J. Chem. Phys. 131 (2009) 181103.
[46] R. Schinke, P. Fleurat-Lessard, J. Chem. Phys. 122 (2005) 094317.
[47] P. Fleurat-Lessard, S.Y. Grebenshchikov, R. Schinke, C. Janssen, D. Krankowsky, J. Chem. Phys. 119 (2003) 4700.
[48] C. Janssen, J. Guenther, D. Krankowsky, K. Mauersberger, J. Chem. Phys. 111 (1999) 7179.
[49] J. Guenther, B. Erbacher, D. Krankowsky, K. Mauersberger, Chem. Phys. Lett. 306 (1999) 209.
[50] C. Janssen, J. Guenther, D. Krankowsky, K. Mauersberger, J. Chem. Phys. 112 (2000) 11109.
[51] C. Janssen, J. Guenther, D. Krankowsky, K. Mauersberger, Chem. Phys. Lett. 367 (2003) 34.
[52] Y.Q. Gao, R.A. Marcus, J. Chem. Phys. 116 (2002) 137.
[53] D. Charlo, D.C. Clary, J. Chem. Phys. 117 (2002) 1660.
[54] D. Charlo, D.C. Clary, J. Chem. Phys. 120 (2004) 2700.
[55] R.A. Marcus, J. Chem. Phys. 121 (2004) 8201.
[56] T. Xie, J.M. Bowman, Chem. Phys. Lett. 412 (2005) 131.
[57] M.V. Ivanov, S.Y. Grebenshchikov, R. Schinke, J. Chem. Phys. 120 (2004) 10015.
[58] M.V. Ivanov, S.Y. Grebenshchikov, R. Schinke, J. Chem. Phys. 130 (2009) 174311.
[59] M.V. Ivanov, R. Schinke, Mol. Phys. 108 (2010) 259.
[60] N. Ghaderi, R.A. Marcus, J. Phys. Chem. B 115 (2011) 5625.
[61] M. Kryvohuz, R.A. Marcus, J. Chem. Phys. 132 (2010) 224304.
[62] M. Kryvohuz, R.A. Marcus, J. Chem. Phys. 132 (2010) 224305.
[63] M.V. Ivanov, R. Schinke, J. Chem. Phys. 122 (2005) 234318.
[64] H. Hippler, R. Rahn, J. Troe, J. Chem. Phys. 93 (1990) 6560.
[65] J. Troe, Chem. Rev. 103 (2003) 4565.
[66] K. Luther, K. Lum, J. Troe, Phys. Chem. Chem. Phys. 7 (2005) 2764.
[67] M.V. Ivanov, R. Schinke, J. Chem. Phys. 124 (2006) 104303.
[68] R.A. Marcus, in: J.R. Sabin, E. Brandas (Eds.), Advances in Quantum Chemistry, vol. 55, Applications of Theoretical Methods to Atmospheric Science, Elsevier Inc., 2008, p. 5.
[69] J. Sehested, O.J. Nielsen, H. Egsgaard, N.W. Larsen, T. Pedersen, L.K. Christensen, M. Wiegell, J. Geophys. Res. 100 (1995) 20979.
[70] J. Sehested, O.J. Nielsen, H. Egsgaard, N.W. Larsen, T.S. Andersen, T. Pedersen, J. Geophys. Res. 103 (1998) 3545.
[71] J. Guenther, D. Krankowsky, K. Mauersberger, Chem. Phys. Lett. 324 (2000) 31.
[72] A.S. Cole, K.A. Boering, J. Chem. Phys. 125 (2006) 184301.
[73] D. Katakis, H. Taube, J. Chem. Phys. 36 (1962) 416.
[74] Y.L. Yung, A.Y.T. Lee, F.W. Irion, W.B. DeMore, J. Wen, J. Geophys. Res. 102 (1997) 10857.
[75] M.J. Perri, A.L. Van Wyngarden, J.J. Lin, Y.T. Lee, K.A. Boering, J. Phys. Chem. A 108 (2004) 7995.
[76] C.A.M. Brenninkmeijer, T. Röckmann, Anal. Chem. 68 (1996) 3050.
[77] D. Hanson, K. Mauersberger, J. Chem. Phys. 85 (1986) 4669.
[78] D. Krankowsky, C. Janssen, K. Mauersberger, J. Geophys. Res. 108 (2003) 4503.
[79] C. Janssen, J. Geophys. Res. Atmos. 110 (2005) 9.
[80] J.C. Ianni, Kintecus, Windows Version 3.962.
[81] S.M. Anderson, F.S. Klein, F. Kaufman, J. Chem. Phys. 83 (1985) 1648.
[82] M.C. Liang, G.A. Blake, Y.L. Yung, J. Geophys. Res. Atmos. 109 (2004) D10308.
[83] M.V. Ivanov, D. Babikov, J. Chem. Phys. 134 (2011) 144107.
[84] M.V. Ivanov, D. Babikov, J. Chem. Phys. 134 (2011) 174308.
[85] B. Luz, E. Barkan, Geochim. Cosmochim. Acta 69 (2005) 1099.
[86] C. Janssen, B. Tuzson, J. Phys. Chem. A 114 (2010) 9709.

K.L. Feilberg obtained her M.Sc. in chemistry at the University of Copenhagen in 2002, and her Ph.D. at the University of Copenhagen in 2005. Her Ph.D. work was a part of the Copenhagen Global Change Initiative (CoGCI). She was a postdoctoral researcher in Prof. Kristie Boering's group at the University of California, Berkeley, where her work was sponsored by FNU and the Carlsberg Foundation. She is currently working in private industry.

A.A. Wiegel received his B.Sc. degree in Chemistry in 2006 from University of Wisconsin, Madison. He is currently working towards a Ph.D. in Physical Chemistry from the University of California, Berkeley. In 2010, he worked at the Institute of Marine and Atmospheric Research at Utrecht University in Utrecht, the Netherlands as a visiting graduate student scholar. His research interests include atmospheric chemistry, experimental chemical kinetics, and photochemical kinetics modeling.

K.A. Boering received her Ph.D. in physical chemistry from Stanford University under the direction of John I. Brauman in 1992. After a postdoctoral fellowship and research associate position at Harvard University with Steven C. Wofsy, she joined the faculty at the University of California, Berkeley in 1998. She is currently The Lieselotte and David Templeton Professor of Chemistry in the Departments of Chemistry and of Earth and Planetary Science. Her research interests include the physical chemistry of isotope effects and their application to atmospheric chemistry and climate change through laboratory experiments, observations from aircraft and high altitude balloons, and atmospheric modeling.